Supporting Information

Cationic complex directed thiostannate layers with excellent proton conduction and photocatalysis properties

Kai-Li Liu[a,b], Ming-Bu Luo[a], Xuechou Zhou[c] and Qipu Lin*[,a]

a. *State Key Laboratory of Structural Chemistry, Fujian Institute of Research on the Structure of Matter, Chinese Academy of Sciences, Fuzhou, Fujian 350002, China.*

b. *University of Chinese Academy of Sciences, Beijing 100049, China.*

c. *School of Life Sciences, Fujian Agriculture and Forestry University, Fuzhou 350002, China.*

E-mail: linqipu@fjirsm.ac.cn

Table of contents

Section S1: Chemical stability

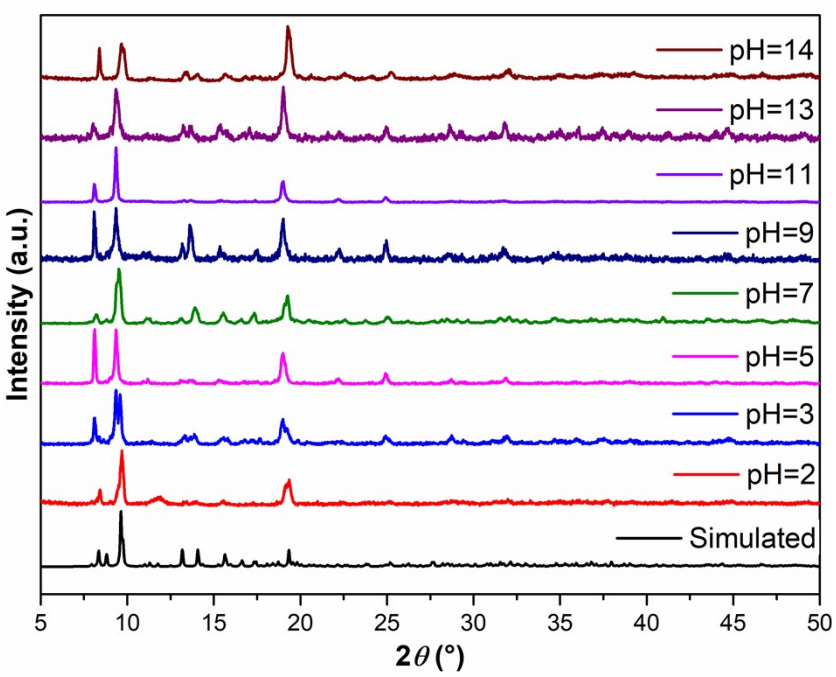

Fig. S1 The PXRD patterns of **SnS-Fe** after immersion in aqueous solution with pH 2-14 for 3 d.

Section S2: Thermogravimetric analysis (TGA)

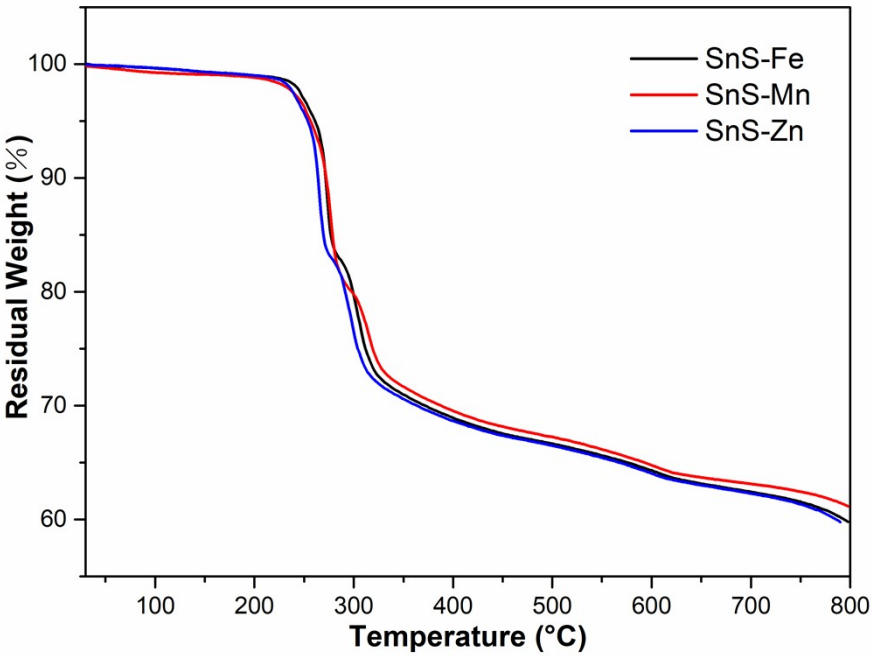

Fig. S2 The TGA curves of **SnS-M** (M = Fe, Mn and Zn).

Section S3: UV-Vis absorption spectra

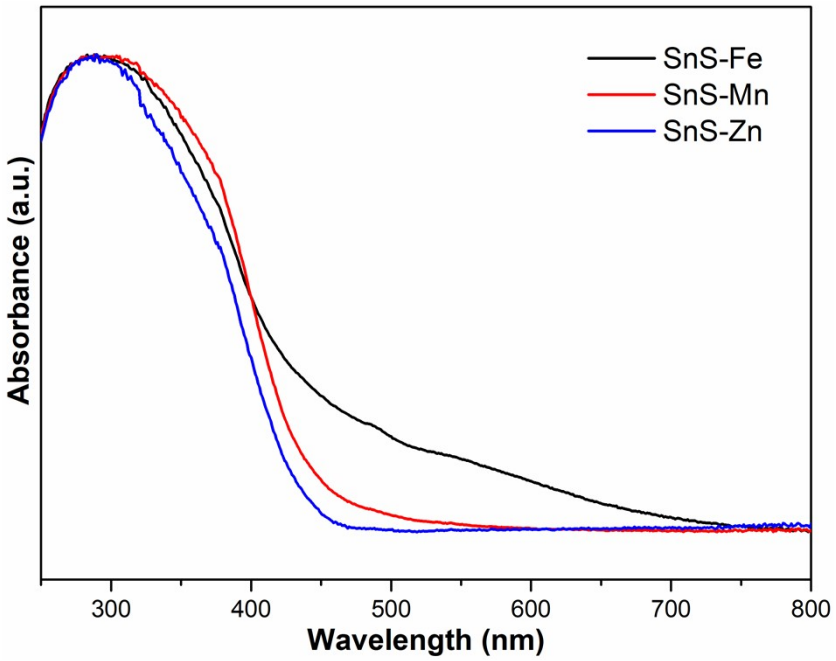

Fig. S3 The UV−Vis absorption spectra of **SnS-M** (M = Fe, Mn and Zn)

Section S4: Mott-Schottky plots

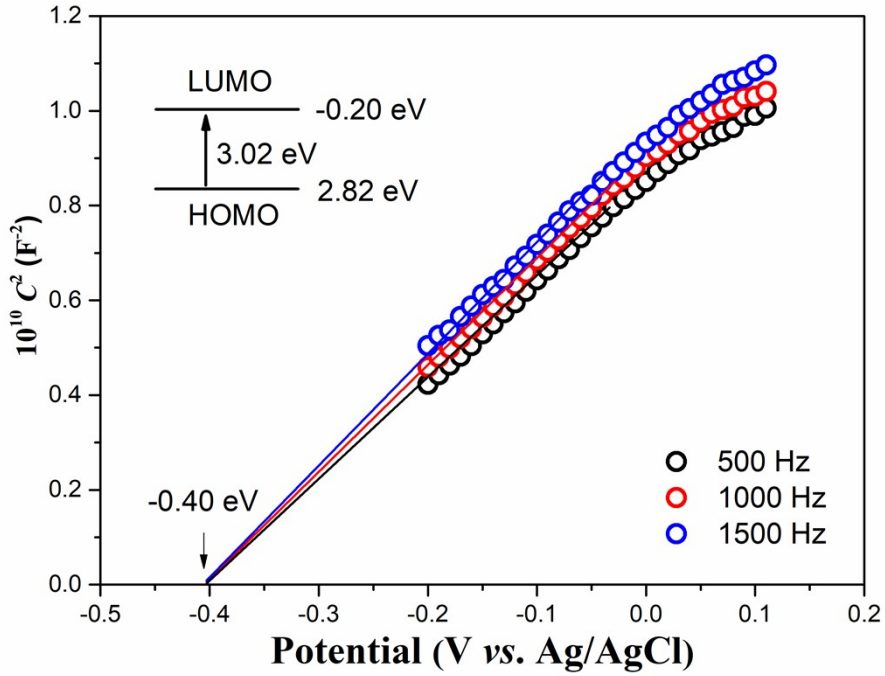

Fig. S4 The Mott-Schottky plots of **SnS-Zn** in 0.2 M Na_2SO_4 solution.

Section S5: Energy dispersive spectroscopy (EDS)

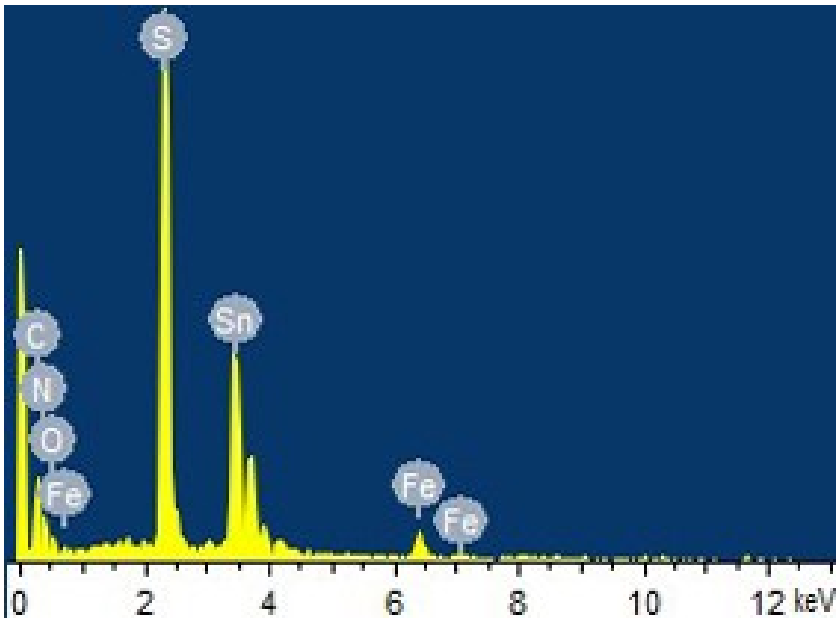

Fig. S5 The EDS plot of **SnS-Fe**.

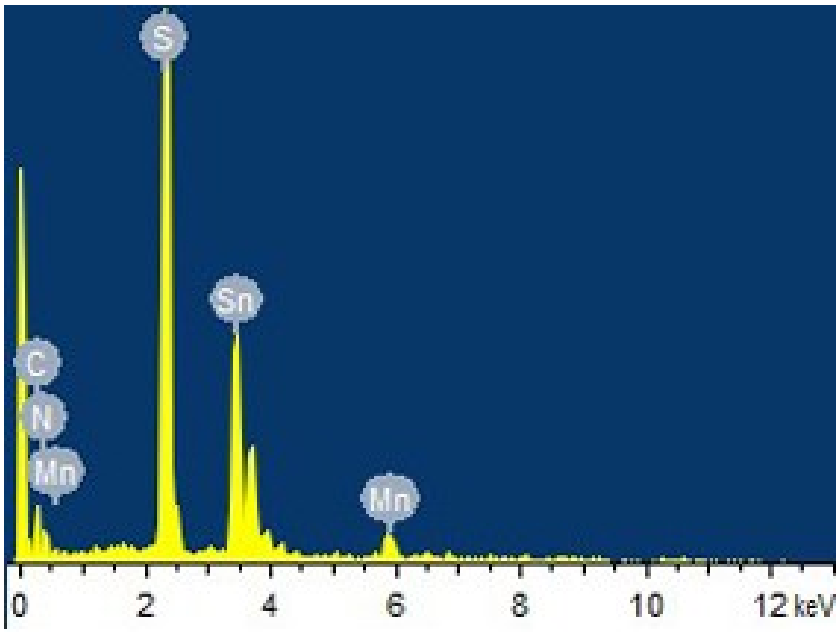

Fig. S6 The EDS plot of **SnS-Mn**.

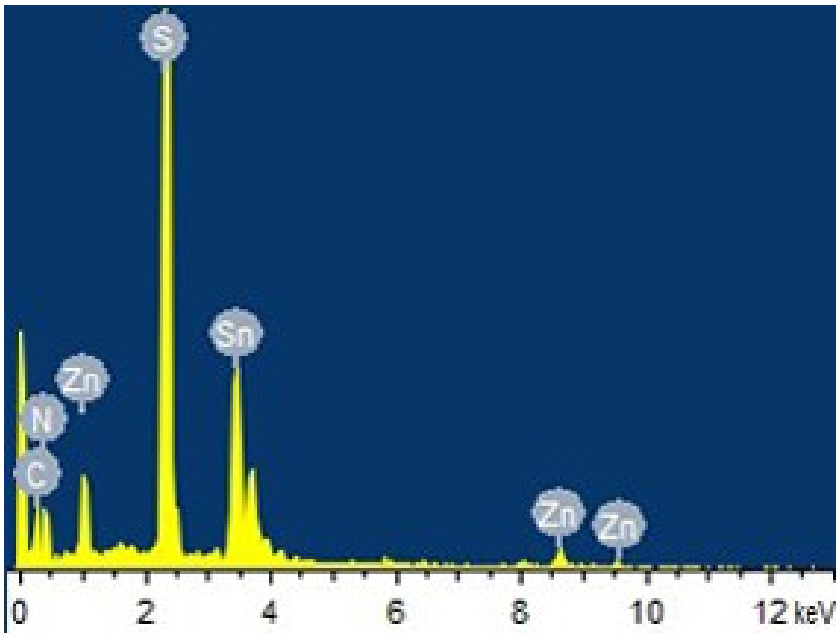

Fig. S7 The EDS plot of **SnS-Zn**.

Section S6: Proton condution

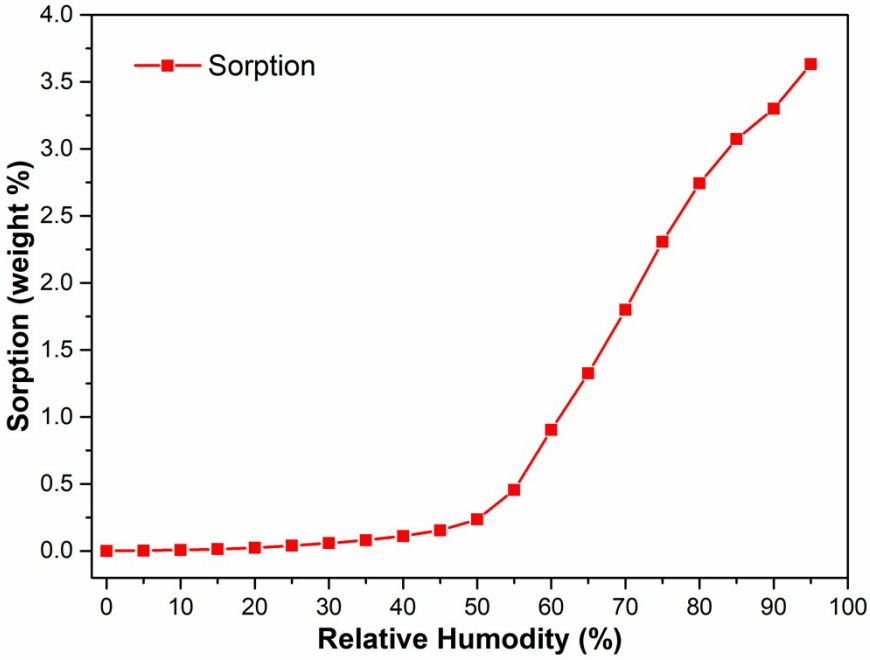

Fig. S8 Water vapor sorption isotherm of **SnS-Fe**.

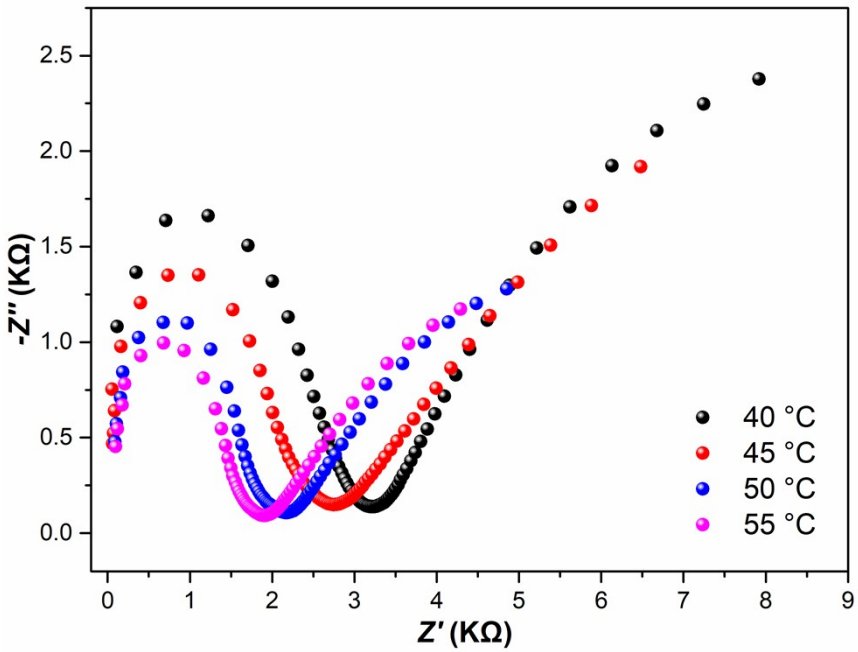

Fig. S9 The Nyquist plots of **SnS-Fe** at different temperatures under 75% rh.

Section S7: Photodegradation

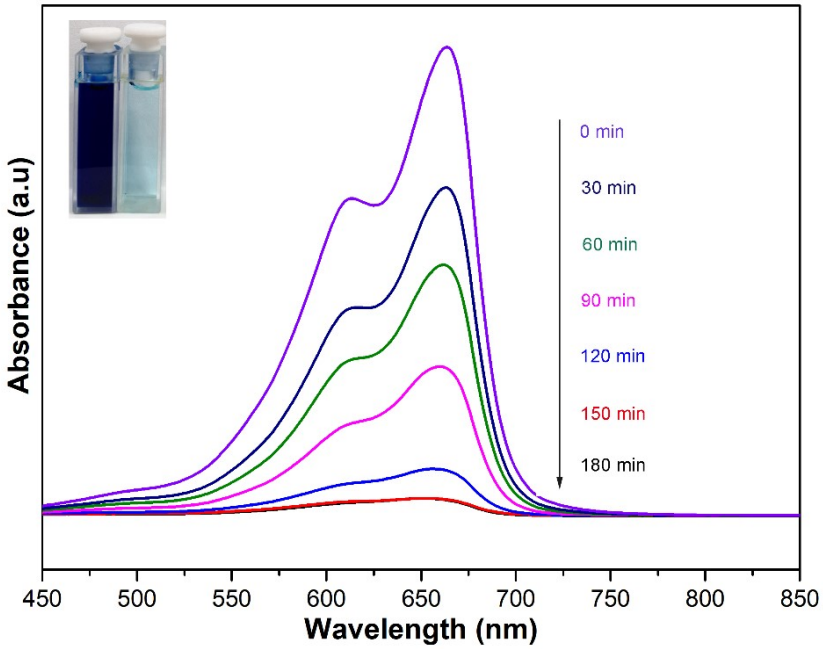

Fig. S10 The time-dependent UV−Vis absorption spectra of MB in the presence of **SnS-Mn** (photodegradation rate, 96.5%).

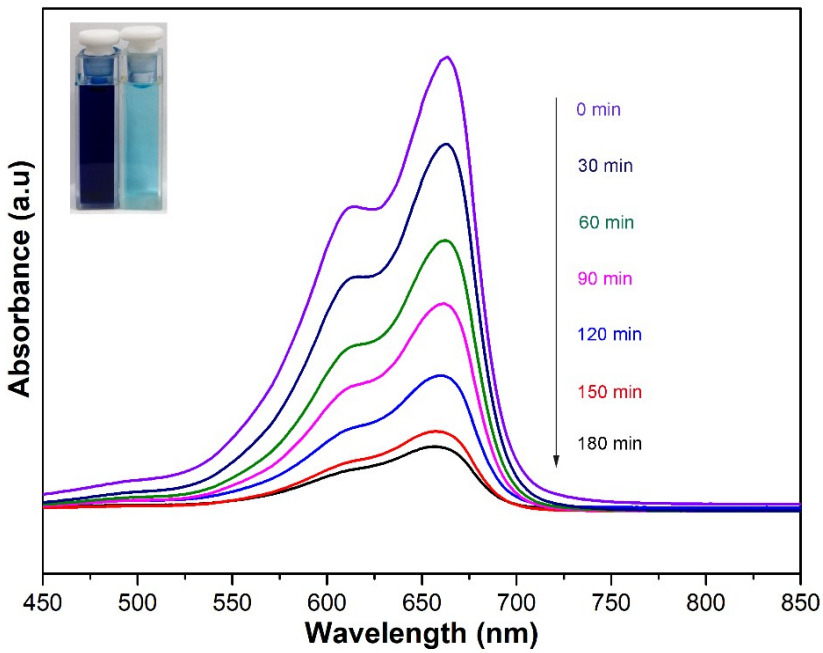

Fig. S11 The time-dependent UV−Vis absorption spectra of MB in the presence of **SnS-Zn** (photodegradation rate, 86.4%).

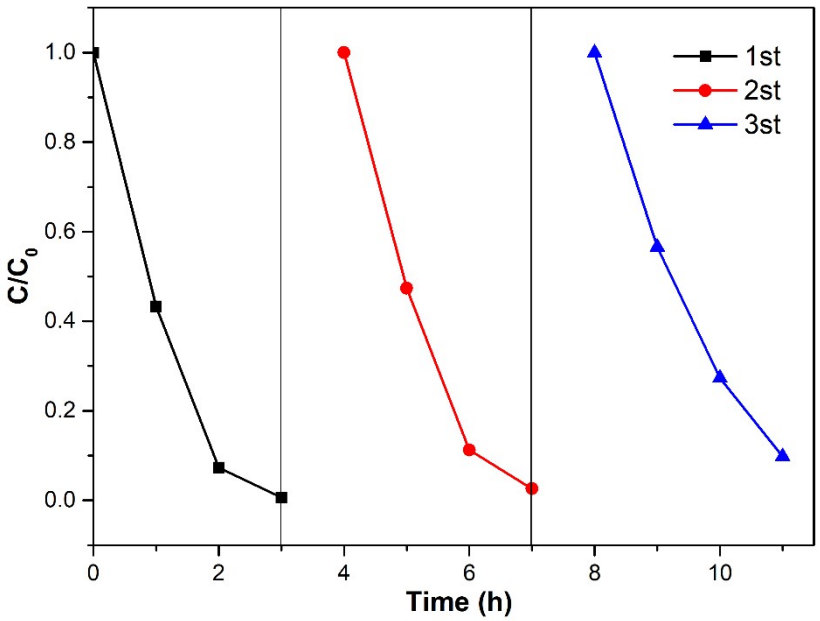

Fig. S12 Photodegradation recycling experiment of **SnS-Fe**.

Section S8: Powder X-ray Diffraction (PXRD)

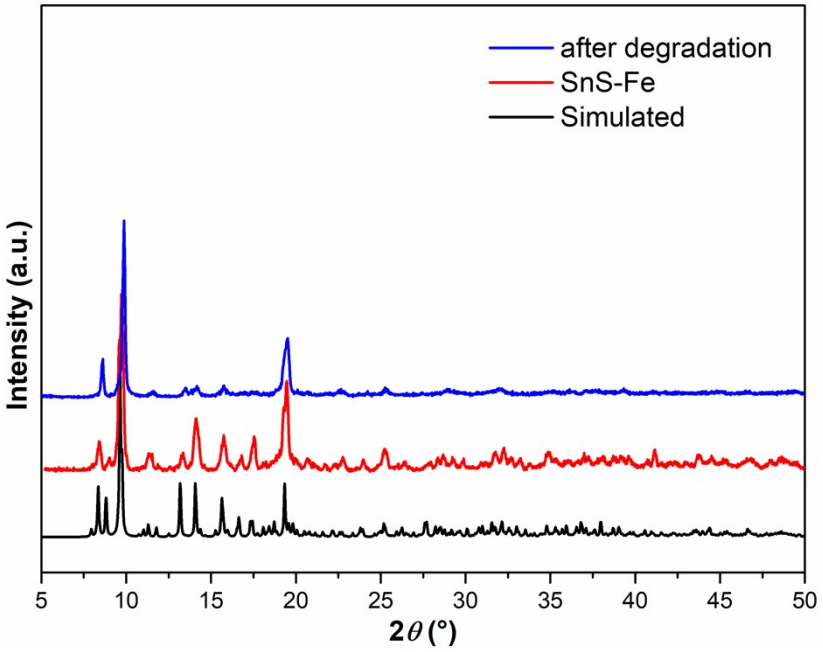

Fig. S13 The simulated and the experimental PXRD patterns of **SnS-Fe** before and after photodegradation experiment.

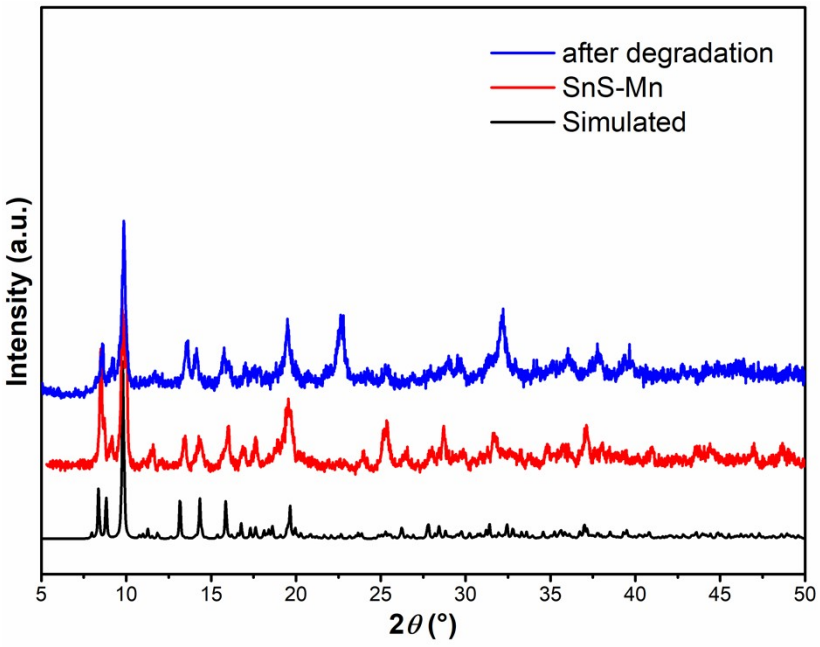

Fig. S14 The simulated and the experimental PXRD patterns of **SnS-Mn** before and after photodegradation experiment.

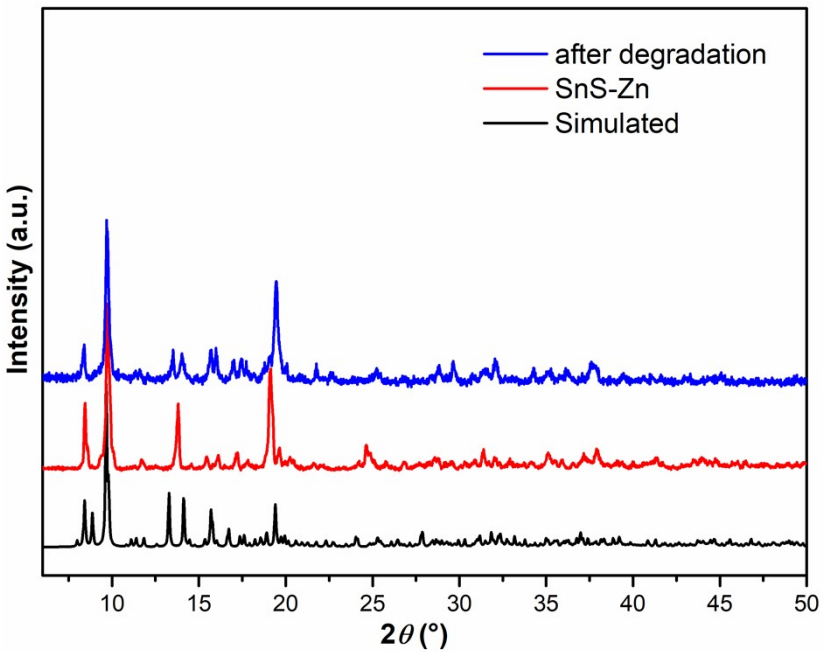

Fig. S15 The simulated and the experimental PXRD patterns of **SnS-Zn** before and after photodegradation experiment.

Section S9: X-ray photoelectron spectroscopy (XPS)

XPS analysis was used to examine the chemical states of the elements in the sample. As shown in **Fig.** S16a, there are Sn, S, Fe, N, C and O species in the **SnS-Fe** both before and after MB photodegradation. Deconvolution of the Fe 2p region (before photodegradation, **Fig.** S16b) by peak fitting showed four main peaks at 714.83, 711.30, 709.61 and 708.15 eV, assigned to Fe^{3+} $2p_{1/2}$, Fe^{2+} $2p_{1/2}$, Fe^{3+} $2p_{3/2}$ and Fe^{3+} $2p_{3/2}$, respectively. After photocatalysis experiment, the peak positions of Fe 2p XPS slightly shifted to higher energy, while the peak area of Fe^{3+} become lower and the peak area of Fe^{2+} become higher after photodegradation, indicating that the electron and hole generated during the photocatalytic process transfered to Fe^{3+}-diethylenetriamine and methylene blue, respectively. The degradation of MB was accompanied by the partial reduction from Fe^{3+} to Fe^{2+} in the Fe-diethylenetriamine complexes. For the Sn 3d region, the slight shifts of the peak positions could be attributed to the interaction between the sample and the absorbed methylene blue. A broad peak of S 2p was found at 163.27 eV indicating the multiple chemical states of S, and the weakening of its signal can be attributed to the partial photocorrosion of the surface chalcogenide species.

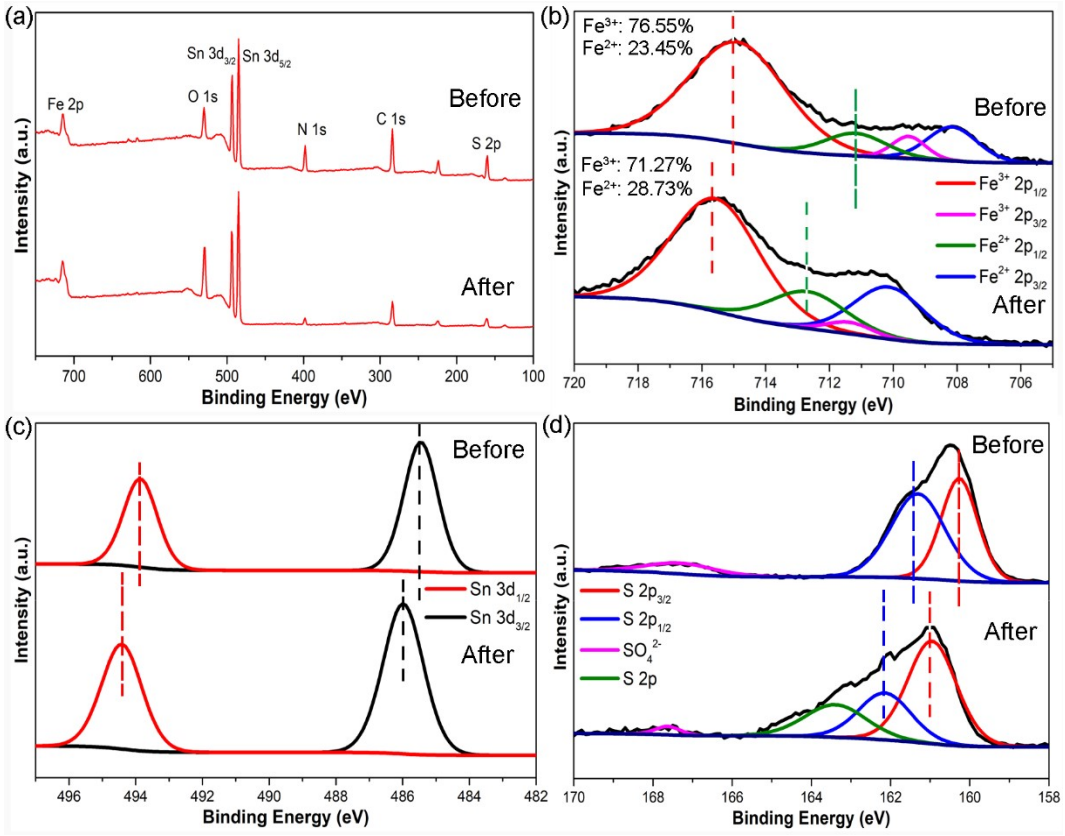

Fig. S16 The XPS analysis of **SnS-Fe** before and after photodegradation of MB including XPS full spectrum (a), Fe 2p (b), Sn 3d (c) and S 2p (d), respectively.